NASA TECHNICAL NOTE

NASA TN D-3286

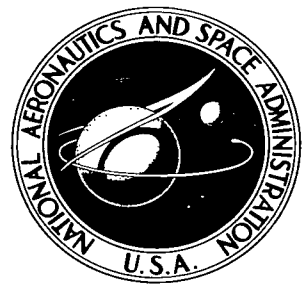

NASA TN D-3286

STUDY OF COAXIAL HALL CURRENT ACCELERATORS AT MODERATE PRESSURES

by H. A. Hassan
North Carolina State University

and

Robert V. Hess and William Grossmann, Jr.
Langley Research Center

NATIONAL AERONAUTICS AND SPACE ADMINISTRATION • WASHINGTON, D. C. • OCTOBER 1966

STUDY OF COAXIAL HALL CURRENT ACCELERATORS AT MODERATE PRESSURES

By H. A. Hassan

North Carolina State University

Robert V. Hess and William Grossmann, Jr.

Langley Research Center
Langley Station, Hampton, Va.

NATIONAL AERONAUTICS AND SPACE ADMINISTRATION

For sale by the Clearinghouse for Federal Scientific and Technical Information
Springfield, Virginia 22151 – Price $2.00

STUDY OF COAXIAL HALL CURRENT ACCELERATORS AT MODERATE PRESSURES

By H. A. Hassan
North Carolina State University

Robert V. Hess and William Grossmann, Jr.
Langley Research Center

SUMMARY

A study of coaxial Hall current accelerators at moderate pressures (of the order of 10 mm Hg) and moderate mass flow rates (of the order of 1 g/sec) is presented. The analysis is based on the conservation equations of the plasma constituents and employs a Saha equation with the gas temperature replaced by the electron temperature. The arc voltage is shown to be a linear function of the applied magnetic field strength at constant total current; also, a voltage plateau is reached at the higher currents for a constant magnetic field strength. In addition, for a given total current, magnetic field strength, pressure, and mass flow rate, the theory predicts the electron, ion, and neutral temperatures; degree of ionization; Hall current; and axial and azimuthal mean velocities. Comparison of theory with experiment shows that the theoretical model is in fair agreement with experiment. The influence of ionization rates and three-dimensional effects is discussed.

INTRODUCTION

Experiments with coaxial Hall current accelerators over a wide range of operating conditions (refs. 1 to 4) show that these devices have certain characteristics in common with the homopolar device (ref. 5). The voltage remains approximately constant, increasing current for a given magnetic field establishing a so-called "voltage plateau," and the increase in voltage with magnetic field for a given current is approximately linear. Since the ionization controls the voltage-current and the voltage—magnetic-field characteristics, the common characteristics could be a result of the fact that the field geometry in the ionization region of the coaxial Hall device is similar to that in the homopolar device.

Even for this similarity in configuration, the theories proposed for the homopolar device, where the mass flow rate is zero, cannot be applied to the coaxial Hall current accelerator, as has been recognized in reference 6. The theory proposed by Alfvén (ref. 5) and extended by Petscheck (ref. 5) and Lin (ref. 7) for the homopolar device is

restricted to the case where the ions as well as the electrons orbit with azimuthal E/B drift velocity where E is the electric field strength and B is the magnetic field strength; thus, azimuthal Hall currents are not permitted to flow. (The possible azimuthal current due to differences of centrifugal effects on ions and electrons is neglected.) It is assumed by Lin that under such conditions, the ion temperature is in excess of the electron temperature and the electrons gain their energy for ionization from the ions. This condition is not in agreement with temperature measurements in coaxial Hall current accelerators at moderate mass flow (ref. 1) as well as at low mass flows (ref. 2) where the electron temperature is considerably in excess of the ion temperature τ_i. Dobryshevskii (ref. 8) shows that excess of ion temperature occurs when $\omega_i \tau_{ia}$ becomes equal to or greater than unity or in the case where the degree of ionization is large. (ω_i is the ion cyclotron frequency and τ_{ia} is the mean time between collision of ions and neutrals.) He bases his theory for the homopolar device on an extension of the theory of the positive column to the case of a discharge in a transverse magnetic field with $\omega_e \tau_{ie} >> 1$ and $\omega_i \tau_{ia} < 1$ (ω_e is the electron cyclotron frequency and τ_{ie} is the mean time between collisions of ions and electrons), whereby the electrons gain their energy directly from the electric field.

Efforts to explain the approximate voltage plateaus and the linear voltage magnetic field characteristics in coaxial Hall accelerators have been made previously by the present authors (refs. 1, 9, and 10) and by Patrick and Schneiderman (ref. 4). The approach used in reference 4 attempts to apply the theory proposed by Alfvén and Petscheck for the homopolar device to the coaxial Hall current accelerator. In this theory the ion slip is assumed to be very large; that is, the interaction of ions and neutrals is negligible and the ions orbit with the E/B drift velocity. It will be shown in the section "Analysis" that the approach used in reference 4 must be modified if the ion slip is moderate and ions are put into rotation progressively along the axis. This modification should be especially important for the acceleration mechanism postulated in the conclusions of reference 4 which are based on acceleration of the neutrals by a small fraction (5 percent) of ions. Furthermore, although the assumption is used that the ion slip is large for the analysis of the voltage-magnetic field strength characteristics, in reference 4 the analysis of the current voltage characteristics is based on considerations which are valid only if the ion slip is small.

It is thus seen that theories for the homopolar device and that of reference 4 for the coaxial Hall device are based on assumptions that are not generally valid in a coaxial Hall current accelerator. The theory presented here (see also refs. 1, 9, and 10) does not depend on the assumption that the ions are orbiting with the drift velocity. It is based on the conservation equations of the plasma constituents that may be derived (for example, ref. 11) from the appropriate Boltzmann equations. The flow is assumed to be steady

and one-dimensional. This assumption implies that the effects of the electrode sheaths are small. Measurements of comparatively small power losses to the electrodes in reference 1 for moderately high mass flows and pressures support this assumption. The conditions under which the electron temperature is expected to be higher than the ion temperature are discussed in detail. It is concluded that for typical operations of coaxial Hall current devices, the electron temperature is always greater than the ion temperature. To keep the numerical complications at a reasonable level, the assumption of local ionization equilibrium has been employed; Saha's equation, the gas temperature being replaced by the electron temperature as suggested by Kerrebrock (ref. 12), is used. Actually, the residence time of particles for various operating conditions of coaxial accelerators is generally less than the time required to reach ionization equilibrium. Although appreciable deviations from ionization equilibrium still exist, even for the higher mass flow rates (ref. 1), the simplified theory still provides a reasonable agreement with experiment. Preliminary results using the rate equation were presented in reference 10.

The calculations were carried out for two and three temperature models and various effective cathode radii. The dependence of the various collision cross sections on temperature was accounted for by using the best available experimental data. As a result of these calculations, the electron, ion, and neutral temperatures, the degree of ionization, the Hall current, the voltage-current, and the voltage-magnetic field characteristics can be predicted for a given magnetic field, total current (or power input), pressure and mass flow rate. It will be shown that regardless of the value of the effective cathode radius, the voltage was a linear function of the magnetic field at a constant current. Also, a voltage plateau is indicated for a constant magnetic field at the higher currents. The other predictions of the theory were in fair agreement with experiment. It is assumed in the analysis that the discharge is uniformly distributed. The transition from spokes to a uniformly distributed discharge has been studied in reference 1 as a function of magnetic field and temperature of the arc-heated thoriated tungsten cathode.

The work done by H. A. Hassan presented herein was done under NASA Grant NsG-363 at North Carolina State University, Raleigh, North Carolina. The analysis presented herein was completed in July 1965.

SYMBOLS

A	cross-sectional area
a	cathode radius
B	magnetic field strength
b	anode radius

D	operator
E	electric field strength
e	electronic charge
g_s	degeneracy of the ground state of species s
H	specific enthalpy
h	Planck's constant
I	ionization potential
i	unit vector
J	total current
j	current density
K	quantity defined by equation (6)
k	Boltzmann constant
ℓ	length of discharge
m	mass of particle
$\dot{m}$	mass flow rate
n	number density of nuclei
n_s	number density of species s
P	power input
p	pressure
Q	rate of heat loss
Q_i	ionization cross section
q	heat flux
R_s	rate of production of species s
r,θ,z	cylindrical coordinates

T	temperature
t	time
t_i	characteristic ionization time
t_r	characteristic residence time
U	mean velocity
u,v	velocity components in directions of z and θ
V	voltage
V_s	velocity of species s
Z_{st}	diffusion cross section
α	degree of ionization
ϵ	energy of internal modes
θ_s	dimensionless temperature of species s
λ	quantity defined by equation (18)
ρ	density
ρ_s	density of species s
σ_o	conductivity in absence of a magnetic field
τ_{st}	mean time between collisions of particles s and t
ω_s	cyclotron frequency of species s

Subscripts:

i,e,a	ion, electron, neutral
s,t	refer to any of the plasma constituents
r,θ,z	refer to cylindrical coordinate system (fig. 1)

An arrow over a symbol denotes a vector quantity.

ANALYSIS

The analysis is based on the conservation equations for the plasma constituents. In spite of the fact that the flow field in a coaxial Hall current accelerator is axisymmetric, with both r and z dependence, it will be assumed, as a first approximation, to be a function of z with r appearing as a parameter. For a steady, one-dimensional flow, the overall continuity equation can be written as

$$\rho u A = \dot{m} \tag{1}$$

where ρ, u, A, and $\dot{m}$ denote, respectively, the mean density, mean axial velocity, cross-sectional area, and mass flow rate. The individual continuity equations for the plasma constituents may be written as

$$\nabla \cdot \left(n_s \vec{V}_s\right) = R_s \tag{2}$$

where n_s, $\vec{V}_s$, and R_s are the number density, velocity, and rate of production in particles per volume of species s, respectively. To avoid the unnecessary complications of dissociation and multiple ionization, only singly ionized monatomic gases are considered. For such gases, ionization is due mainly to electron-neutral collisions; that is, the dominant reaction is

$$A + e \rightarrow A^+ + e + e \tag{3}$$

Opposing this reaction is the recombination reaction

$$A^+ + e + e \rightarrow A + e \tag{4}$$

In equations (3) and (4), A denotes the atom; A^+, the ion; and e, the electron. Based on these reactions, R_s can be expressed as

$$R_s = R_e = R_i = -R_a = \left(n_e n_a - \frac{n_i n_e^2}{K}\right) f(T_e) \tag{5}$$

where

$$K = 2\frac{g_i}{g_a}\left(\frac{2\pi m_e k T_e}{h^2}\right)^{3/2} \exp\left(-\frac{I}{kT_e}\right) \tag{6}$$

and (from ref. 13)

$$f(T_e) = \left(\frac{8}{\pi m_e}\right)^{1/2}\left(\frac{1}{kT_e}\right)^{3/2} \int_I^\infty \exp\left(-\frac{\xi}{kT_e}\right) Q_i(\xi)\, \xi\, d\xi \tag{7}$$

where g_i, g_a are the degeneracies of the ground states of the ions and atoms; m_e, the mass of the electron; ξ, dummy variable, k, the Boltzmann constant; h, Planck's constant; I, the first ionization potential; T_e, the electron temperature; and Q_i is the ionization cross section. If the diffusion velocity is small compared with the mean velocity, that is, if

$$\vec{V}_s \approx \vec{U} \tag{8}$$

where $\vec{U}$ is the mean velocity, equation (2) gives for a one-dimensional flow

$$nu\frac{d\alpha}{dz} = R_s \tag{9}$$

where α is the degree of ionization defined by

$$\left.\begin{aligned} n_e = n_i = \alpha n \\ n_a = (1 - \alpha)n \end{aligned}\right\} \tag{10}$$

and n is the number density of the nuclei and where the gradient of the diffusion velocity is assumed to be small.

Because of the complexity of equation (9), the question arises whether a simpler equation can be employed to calculate the degree of ionization. Examination of equations (5) and (9) shows that a characteristic ionization time can be defined as

$$t_i = \frac{n}{n_e n_a f(T_e)} \tag{11}$$

Thus, t_i is small if $f(T_e)$ is large. This characteristic time may be compared with a typical residence time t_r. For the case where

$$\frac{t_i}{t_r} < 1 \tag{12}$$

ionization equilibrium is attained in the chamber; in this case

$$n_e n_a \approx \frac{n_i n_e^2}{K}$$

or

$$\frac{\alpha^2}{1 - \alpha} = \frac{K}{n} \tag{13}$$

which is Saha's equation. On the other hand, if $\frac{t_i}{t_r} > 1$, ionization equilibrium is not attained in the chamber and equation (9) has to be employed. It is expected that for the higher mass flow rates and the higher pressures, equation (13) can be employed. This procedure was followed for the case of moderate mass flows for the sake of simplicity.

The momentum equations give, in addition to the expressions for the mean velocities, the ion and electron current densities. If the coupling between diffusion and heat flux is ignored, one can use the expressions derived by Cowling (ref. 14) for the ion current density and the total current density. Assuming that collision cross sections of charged particles are much larger than cross sections of collisions involving neutral atoms and solving Cowling's expressions explicitly for the current densities yields

$$\vec{j} = \frac{\sigma_o}{\omega_e \tau_{ie}(1 + \lambda^2)} \left\{ \lambda \left[\vec{E}^* - \left(\frac{\vec{E} \cdot \vec{B}}{B^2} \right) \vec{B} \right] - \frac{\vec{E}^* \times \vec{B}}{B} \right\} + \sigma_o \left(\frac{\vec{E} \cdot \vec{B}}{B^2} \right) \vec{B} \tag{14}$$

and

$$\vec{j}_i = \left[\lambda - \left(\omega_e \tau_{ie} \right)^{-1} \right] \frac{\vec{j} \times \vec{B}}{B} \tag{15}$$

with

$$\vec{j} \times \vec{B} = \frac{\sigma_o}{\omega_e \tau_{ie}(1 + \lambda^2)} \left[\lambda \left(\vec{E}^* \times \vec{B} \right) + B\vec{E}^* - \left(\frac{\vec{E} \cdot \vec{B}}{B} \right) \vec{B} \right] \tag{16}$$

$$\vec{j} = \vec{j}_e + \vec{j}_i \tag{17}$$

$$\lambda = \left(\omega_e \tau_{ie} \right)^{-1} + 2(1 - \alpha)^2 \omega_i \tau_{ia} \tag{18}$$

$$\left. \begin{aligned} \vec{E}^* &= \vec{E} + \vec{U} \times \vec{B} \\ \sigma_o &= \frac{n_e e^2 \tau_{ie}}{m_e} \end{aligned} \right\} \tag{19}$$

$$\left. \begin{aligned} \omega_s &= \frac{eB}{m_s} \\ \tau_{st} &= \frac{3}{2\left[2k \left(\frac{T_s}{m_s} + \frac{T_t}{m_t} \right) \right]^{1/2} n_t Z_{st}} \end{aligned} \right\} \tag{20}$$

where $\vec{E}$, $\vec{B}$, and Z_{st} denote, respectively, the electric fields, magnetic field, and diffusion cross section.

If viscous stresses are neglected, the overall momentum equation can be expressed as

$$\left.\begin{aligned} \rho\left(\frac{D\vec{U}}{Dt}\right) + \nabla p &= \vec{j} \times \vec{B} \\ p = \sum p_s &= \sum k n_s T_s \end{aligned}\right\} \tag{21}$$

where p is the pressure. In the arc region of a coaxial accelerator, a crossed-field geometry with an axial magnetic field and a radial electric field is assumed. Thus, in the region under consideration,

$$\vec{U} = \vec{i}_z u + \vec{i}_\theta v \tag{22}$$

$$\vec{j} = -\vec{i}_r j_r - \vec{i}_\theta j_\theta \tag{23}$$

$$\left.\begin{aligned} \vec{B} &= \vec{i}_z B \\ \vec{E} &= -\vec{i}_r E \end{aligned}\right\} \tag{24}$$

The components of equations (21) in the z- and θ-directions can be expressed as

$$\rho u \frac{du}{dz} + \frac{dp}{dz} = 0 \tag{25}$$

and

$$\rho u \frac{dv}{dz} = j_r B \tag{26}$$

Also, use of equations (22) to (24) in equation (14) yields

$$j_r = \frac{\sigma_o \lambda}{\omega_e \tau_{ie}(1 + \lambda^2)}(E - vB) \tag{27}$$

and

$$j_\theta = \frac{j_r}{\lambda} \tag{28}$$

If one chooses

$$j_r = \frac{J}{2\pi r l} \tag{29}$$

where J is the total current and l is the length of the region over which the discharge extends, the charge conservation equation

$$\nabla \cdot \vec{j} = 0 \tag{30}$$

is satisfied. The independence of j_r with respect to z was chosen to keep the analysis simple. If one had assumed instead independence of E with respect to z, the variation of j_r with z would have to be considered. The total current J applied over a length l would then have to be expressed in the more general form than equation (29); that is,

$$J = 2\pi r \int_0^l j_r \, dz \tag{30a}$$

The limitations of the assumptions regarding the field geometry and the one-dimensional approximation can be seen from equations (26), (27), and (29). Equation (29) shows that the properties are functions of r in addition to being functions of z. This condition would indicate that for axisymmetric devices, the one-dimensional approximation may be rather crude, especially in the regions where derivatives with respect to r cannot be ignored. Also, for constant cross-sectional area, equation (26) can be readily integrated to yield

$$v = \frac{A}{\dot{m}} B \int_0^z j_r \, dz \tag{31}$$

where for the case of j_r independent of z, using equation (29) yields

$$v = \frac{A}{\dot{m}} B \frac{J}{2\pi r} \frac{z}{l} \tag{31a}$$

It is indicated from equations (27) and (31a) that if constant current density j_r is to be maintained with increasing z, the electric field would have to increase with z to prevent v from exceeding $\frac{E}{B}$. Since the variation of E_r with z is small in the present experiments, the simplified analysis using j_r independent of z is restricted to values of v small compared with $\frac{E}{B}$. Experimental evidence obtained in reference 1 indicates that this approximation is good for the moderate mass flows. Since for low mass flow used in electric propulsion a wide variety of electrode configurations exists, which have different distributions of E_r and j_r, a variety of distributions is being studied in order to permit comparison with experiments.

Three energy equations are needed to determine the electron, ion, and neutral temperatures. These energy equations may be taken as the overall energy equation and two of the species energy equations. If viscous dissipation is ignored, the overall energy equation may be written as

$$\rho \frac{D}{Dt}\left(H + \frac{U^2}{2}\right) + \nabla \cdot \vec{q} - \vec{E} \cdot \vec{j} = 0 \tag{32}$$

where

$$H = \frac{1}{\rho}\left(\frac{5}{2}\sum kn_s T_s + In_e\right)$$

is the specific enthalpy and $\vec{q}$ is the heat flux vector. The species energy equations can be expressed as (ref. 11)

$$\frac{d}{dz}\left[un_s\left(\frac{3}{2}kT_s + \epsilon_s\right)\right] + p_s\frac{du}{dz} + \frac{dq_s}{dz} = \vec{E}^* \cdot \vec{j}_s - 3\sum K_{st}\frac{k(T_s - T_t)}{m_s + m_t} \tag{33}$$

where

$$K_{st} = \frac{2}{3}\frac{m_s m_t}{m_s + m_t}\sqrt{2k\left(\frac{T_s}{m_s} + \frac{T_t}{m_t}\right)}Z_{st}n_s n_t \tag{34}$$

where

$$\left.\begin{aligned} \epsilon_a &= 0 \\ \epsilon_i &= I \qquad (\epsilon_e = 0) \\ \epsilon_e &= I \qquad (\epsilon_i = 0) \end{aligned}\right\} \tag{35}$$

and q_s is the heat flux vector of species s. Since the mass of the atom is almost equal to the mass of the ion, the assumption is usually made that the ion and neutral temperatures are equal. As a result of this assumption, only equation (32) and one of equations (33) are needed.

To complete the formulation of the problem, expressions for the various collision cross sections are needed. The ion-electron cross section is obtained by assuming that

the ion-electron collisions follow Coulomb's law. In this case, however, the resulting expression depends on the cut-off distance. If the suggestion of Spitzer (ref. 15) is used, for argon,

$$Z_{ie} = 2.96 \times 10^{-16} \theta_e^{-2} \log_e \left[3.441 \times 10^6 \left(\frac{\theta_e^3}{n_e} \right)^{1/2} \right] \tag{36}$$

where

$$\theta_s = \frac{kT_s}{I} \tag{37}$$

The electron-neutral collision cross section for argon was obtained from the data of Massey and Burhop, Barbiere, and Frost and Phelps (refs. 16 to 18). For electron temperatures of the order of 1.0 eV, the cross section has a minimum as a result of the Ramsauer-Towsend effect; whereas for electron temperatures of the order of 10.0 eV, the cross section has a maximum. By using the data of references 16 to 18, the cross section was approximated by the quadratic expressions,

$$Z_{ea} = 0.16 \times 10^{-16} + 5.015 \times 10^{-14} (\theta_e - 0.01585)^2 \tag{38a}$$

and

$$Z_{ea} = 15.835 \times 10^{-16} - 32.390 \times 10^{-16} (\theta_e - 0.812440)^2 \tag{38b}$$

The data on ion-neutral collision cross sections for argon have been summarized by Fay (ref. 19). For temperatures less than 1000° K, the polarization force is important; whereas for higher temperatures, short-range forces are dominant. Since it is anticipated that ion temperatures higher than 1000° K exist in discharges of interest, it is assumed here that ion-neutral collisions follow the Lennard-Jones potential. At the higher temperatures, the repulsive part of the potential is dominant; therefore, for argon (ref. 20),

$$Z_{ia} = 2.528 \times 10^{-15} \left(\frac{\theta_i + \theta_a}{2} \right)^{-1/6} \tag{39}$$

It should be noted that values of Z_{ia} based on charge exchange are more appropriate. However, the results were practically unchanged for values one order of magnitude higher than those in equation (39).

In problems of arc discharges, it is desired to calculate the arc properties for a given power input or a given total current. Since

$$P = JV \tag{40}$$

where V is the voltage, an expression for V is needed. Equations (27), (30), and (31) give

$$E = \frac{\omega_e \tau_{ie}}{\sigma_o} \frac{1 + \lambda^2}{\lambda} \frac{J}{2\pi r l} + \frac{A}{\dot{m}} \frac{JB^2}{2\pi r} \frac{z}{l} \tag{41}$$

Since E_z is assumed to be zero, V is given by

$$V = \int_a^b E \, dr \tag{42}$$

where a is the effective cathode radius and b is the anode radius. Equations (41) and (42) show that V depends on z; therefore, the assumption that $E_z = 0$ is an approximation if j_r cannot vary with z. Also, since the flow properties depend on r implicitly, integration of equation (42) requires the solution of the one-dimensional equations for different values of r. In view of the assumptions introduced here, such a procedure is not warranted. Therefore, it is assumed that the dependence of E on r is one of proportionality to $\frac{1}{r}$; hence,

$$V \approx \left(\frac{\omega_e \tau_{ie}}{\sigma_o} \frac{1 + \lambda^2}{\lambda} \frac{J}{2\pi l} + \frac{A}{\dot{m}} \frac{JB^2}{2\pi} \right) \log_e \frac{b}{a} \tag{43}$$

In the evaluation of expression (43), z was chosen to be equal to l.

Examination of equation (43) shows that the voltage depends explicitly on the three parameters a, b, and l. Of these parameters, only b is probably well defined; it is usually chosen as the actual geometric radius of the anode. Determining the effective cathode radius is a very difficult theoretical and experimental problem, and current bulging makes it very difficult to determine l. The situation is made more difficult because a and l vary with J and B. Since a one-dimensional theory cannot predict a and l, these parameters are to be treated as experimentally determined parameters.

From equations (30) and (42), the volume integral of equation (32) can be written as

$$\dot{m} \left[H + \frac{U^2}{2} - \left(H + \frac{U^2}{2} \right)_o \right] = JV \frac{z}{l} - Q \tag{44}$$

where the subscript o denotes conditions at the chamber entrance and Q is the rate of heat loss. In obtaining the volume integral, the assumption was made that E_r and V are independent of z; the total current J, as indicated in equation (30a), is, however,

independent of the variation of j_r with z. Equation (44) is valid regardless of any other assumptions regarding ionization rates or any other assumptions employed in deriving equation (14).

THE CONSTANT-PRESSURE APPROXIMATION

The geometry of the channel and of the field configuration chosen here limits the Mach number to a maximum of unity. It is expected that in the regions where the Mach number is less than one, most of the energy supplied to the arc goes into ionization. Because a small fraction is going into acceleration, the assumption of constant pressure in the arc region is somewhat justified. As a result of this assumption, the axial velocity is calculated from equation (1) and is

$$u = \frac{\dot{m}}{\rho A} = \text{Constant} \tag{45}$$

The electron energy equation can be simplified from the consideration that the electrons lose very little of their energy in a given collision. This condition would imply that terms containing the electron temperature gradient may be considered to be small compared with the power input and collision terms. Introducing this assumption into equation (33) and assuming negligible effects of inelastic collisions yields

$$\vec{E}^* \cdot \vec{j}_e = 3 \sum K_{et} \frac{k(T_e - T_t)}{m} \qquad (m = m_a \approx m_i) \tag{46}$$

The Two-Temperature Analysis

Because the mass of the atom is almost equal to that of the ion, the assumption is usually made that the ion temperature is equal to the atom temperature. As a result of this assumption, two energy equations are needed and these equations may be chosen as equations (44) and (46). Choice of equation (46) as the second energy equation shows that the electron temperature is always greater than the atom or neutral temperatures. This condition is not in agreement with the ionization mechanism advanced by Lin (ref. 7), in which he assumed an ion temperature in excess of the electron temperature.

It is seen from equation (33) that in the situations where pressure and temperature gradients and inertia terms are small compared with power inputs and collision terms, choice of the ion energy equation, which in this case reduces to

$$\vec{E}^* \cdot \vec{j}_i = 3 \sum K_{it} \frac{k(T_i - T_t)}{m + m_t} \tag{47}$$

would lead to an ion temperature in excess of the electron temperature, a result that is in agreement with Lin's assumption. As a result, the assumptions $T_i = T_a$ and steady uniform (gradients negligible) plasma are not compatible. Also, the choice of equation (46) and not equation (47) as the second energy equation should be justified.

The choice of the appropriate energy equation can be inferred from a comparison of the terms containing the temperature gradients and the power input terms in equation (33). As has been pointed out, the electrons lose very little of their energy in their collisions with the ions and atoms. On the other hand, because the mass of the ion is almost equal to that of the atoms, the ions lose an appreciable part of their energy when they collide with the atoms. Thus, since collision of electrons with the heavier particles is characterized by longer relaxation times, it is expected that $|DT_e/Dt| < |DT_i/Dt|$. The power received by the ions and electrons can be calculated by employing equations (14) and (15). For the configuration under consideration,

$$\vec{j}_i \cdot \vec{E}^* = \frac{\sigma_o}{\omega_e \tau_{ie}(1 + \lambda^2)}\left[\lambda - (\omega_e \tau_{ie})^{-1}\right]E^{*2}$$

and

$$\vec{j}_e \cdot \vec{E}^* = \frac{\sigma_o}{(\omega_e \tau_{ie})^2(1 + \lambda^2)} E^{*2} \tag{48}$$

Hence,

$$\frac{\vec{j}_i \cdot \vec{E}^*}{\vec{j}_e \cdot \vec{E}^*} = 2(1 - \alpha)^2 \omega_e \tau_{ie} \omega_i \tau_{ia} \tag{49}$$

Thus, in situations where the ratio (eq. (49)) is of order unity or less, equation (46) is the appropriate equation. On the other hand, if the ratio (eq. (49)) is much greater than unity, use of equation (46) may be in error. In such case, use of equation (47) is more appropriate provided that terms containing dT_i/dz are small compared with $\vec{j}_i \cdot \vec{E}^*$.

Most operating conditions of existing coaxial Hall current accelerators are such that $2(1 - \alpha)^2 \omega_i \tau_{ia} \omega_e \tau_{ie} < 1$. Hence, use of equation (46) is justified in this work. Since this discussion did not take into consideration inelastic collisions and radiation losses, these conclusions are expected to be valid for electron temperatures of the order of 2.0 to 3.0 eV or less.

The Three-Temperature Analysis

The relation between the ion and electron temperatures in a steady and uniform (negligible gradients) plasma can be investigated by utilizing equations (46) and (47).

Solving these equations for $T_e - T_a$ and $T_i - T_a$ yields

$$T_e - T_a = \frac{n_i Z_{ie} \vec{E}^* \cdot \vec{j} + \delta n_a Z_{ia} \vec{E}^* \cdot \vec{j}_e}{\beta \Delta} \tag{50}$$

and

$$T_i - T_a = \frac{n_e Z_{ie} \vec{E}^* \cdot \vec{j} + n_a Z_{ae} \vec{E}^* \cdot \vec{j}_i}{\beta \Delta} \tag{51}$$

where

$$\beta = 2\left(\frac{k}{m}\right) m_e \sqrt{\frac{2kT_e}{m_i}}\, n_i$$

$$\delta = \frac{1}{4}\left(\frac{m}{m_e}\right)^{1/2} \sqrt{\frac{T_i + T_a}{T_e}}$$

and

$$\Delta = n_i n_a Z_{ie} Z_{ae} + \delta n_a Z_{ia}(n_i Z_{ie} + n_a Z_{ae}) \tag{52}$$

It is seen from equations (50) and (51) that $T_e > T_i$ if

$$\delta\left(\frac{Z_{ia}}{Z_{ae}}\right)\left(\frac{\vec{E}^* \cdot \vec{j}_e}{\vec{E}^* \cdot \vec{j}_i}\right) > 1 \tag{53}$$

or, if equations (49) and (52) are used, equation (53) can be written as

$$\frac{1}{4}\left(\frac{m}{m_e}\right)^{1/2} \sqrt{\frac{T_i + T_a}{T_e}}\, \frac{Z_{ia}}{Z_{ae}} > 2(1 - \alpha)^2 \omega_i \tau_{ia} \omega_e \tau_{ie} \tag{54}$$

since $Z_{ia}/Z_{ae} \approx 10^2$ and $T_e > T_i$ for all practical purposes. This analysis gives added support to the considerations justifying the use of equation (46) in the two-temperature analysis. This result is limited to the case where $\omega_i \tau_{ia} \leq 1$. It should be noted that this result is independent of the magnitude of v.

RESULTS AND DISCUSSION

The plasma properties at a given section can be determined from the simultaneous solution of equations (13), (44), and (46) in conjunction with equations (31), (43), and (45). For the three-temperature analysis, these equations have to be supplemented by equation (47). The results of these calculations for a given total current J, magnetic flux density B, mass flow rate and pressure give the electron, ion, and neutral temperatures, the axial and azimuthal velocity, the voltage, and Hall current.

As has been pointed out, the quantities r, a, b, and l are constants which have to be specified for any given calculation. In this work, various values of r and a have been chosen; however, no effort has been made to vary b and l. Since most of the ionization is expected to take place near the plane of the cathode tip, a does not correspond to the radius of the cathode cylinder. (See fig. 1.) The values of a selected ranged from constants independent of J and B to parameters depending on B. In particular, it has been found that, for this investigation, a choice of a as

$$a = 0.02\left[-1 + 10\left(\frac{B}{3000}\right) - \left(\frac{B}{3000}\right)^2\right] \text{cm} \tag{55}$$

over the range of B from 3000 gauss to 9000 gauss results in a reasonable fit of the experimentally measured voltage. The values of r investigated consisted of constants and values determined by the relation

$$r = \frac{a + b}{2} \tag{56}$$

with a given by equation (55). By using various values of r, one can assess, in a very crude way, the importance of three-dimensional effects.

The calculations were carried out for the accelerator shown in figure 1. The device has an anode radius $b = 1.5204$ cm and the cathode cylinder has a radius of 0.899 cm. In the calculations reported here, the mass flow rate was kept constant at 1.8 g/sec, the pressure varied from 10 to 19 mm Hg and l was chosen as 1 cm. All the calculated values shown in the figures correspond to $Q = 0$ and the station $z = l$ where the measurements were made. Heat losses were ignored because the measurements of reference 1 showed that they were small compared with the power input.

The predictions of the three-temperature and the two-temperature analyses were almost identical. This similarity may be attributed to two reasons. As can be seen from figure 2, the calculated T_i and T_a are very close to each other. Also, the range of input parameters considered here was such that the calculated value of

$2(1 - \alpha)^2 \omega_e \tau_{ie} \omega_a \tau_{ia}$ was always less than 1. It may be recalled that this criterion was derived in trying to justify the use of equation (46) as the proper second energy equation in the two-temperature analysis.

Figures 3 and 4 show a plot of the variation of voltage with magnetic field intensity for various values of a and r for a total current of 100 amperes. The figures show that regardless of the values of a or r, the voltage increases linearly with B at constant total current. The various interpretations for the linear V - B relationship in homopolar devices and coaxial Hall current accelerators were reviewed in the introduction. It was concluded then that the assumptions employed by the various investigators were not applicable to the coaxial Hall current accelerator. It may be recalled that the analysis presented here assumes that the electrons receive most of the energy from the electric field with the result that the electron temperature is in excess of the ion temperature in accordance with experiment. Also, Hall currents, which play an important role in coaxial Hall current devices, are included. In an effort to find out the reasons for the results shown in figures 3 and 4, attention is directed to equation (46) and references 9 and 10. When equations (19), (20), (34), and (48) are used, equation (46) can be written as

$$\frac{1}{1 + \lambda^2}\left(\frac{E^*}{B}\right)^2 = 3\frac{I}{m}\left(1 + \frac{1 - \alpha}{\alpha}\frac{Z_{ea}}{Z_{ei}}\right)(\theta_e - \theta_i) \tag{57}$$

The results of the calculations showed that for the range of J and B considered, 100 amperes to 300 amperes and 3000 gauss to 10 500 gauss, respectively, $v < E/B$, $\theta_i < \theta_e$, and λ and θ_e are "weak" functions of B at constant J. Thus, approximately, equation (57) can be written as

$$\frac{E}{B} = \sqrt{3\frac{I}{m}\left(1 + \frac{1 - \alpha}{\alpha}\frac{Z_{ea}}{Z_{ei}}\right)(1 + \lambda^2)\theta_e} = c\sqrt{2\frac{I}{m}} \qquad (c \approx \text{Constant}) \tag{58}$$

where, for the conditions analyzed in this work, c was less than unity. The fact that λ is a weak function of B is a result of taking into consideration the ion slip term; otherwise, the validity of equation (58) would require $\omega_e \tau_{ie} \gg 1$ or $\lambda \ll 1$. Equation (57) shows also that the limit of E as B approaches zero exists. Denoting this limit by E_o yields

$$E_o = \frac{m_e}{e\tau_{ie}}\sqrt{3\frac{I}{m}\left(1 + \frac{1 - \alpha}{\alpha}\frac{Z_{ae}}{Z_{ei}}\right)(\theta_e - \theta_i)} \tag{59}$$

The fact that the linear V - B characteristic of constant current exists for

$$v < \frac{E}{B} = c\sqrt{2\frac{I}{m}} \qquad (c < 1) \qquad (60)$$

shows that the linear V - B characteristic is not dependent on the ions drifting with the critical velocity $\sqrt{2\frac{I}{m}} = \frac{E}{B}$ as indicated in reference 4, based on discussion of the homopolar device in references 5 and 7.

At the lower mass flow rates, the quantity c could conceivably be of order unity because of the high electron temperature observed. This condition would explain the experimental results of the low mass flow devices observed in references 2 and 4. As stated at the end of the section "The Two-Temperature Analysis" for electron temperatures in excess of 2.0 eV to 3 eV, the effects of inelastic collisions and radiation losses would have to be included.

The calculations for moderate mass flows have been also carried out with an electron energy equation which took into consideration the heat loss by radiation and the inelastic collisions. Both of these contributions were found to have negligible effects on the results. The possible influence of losses to the electrodes is being evaluated in detail.

Figure 3 also shows the sensitivity of the voltage to the effective cathode radius. In this connection, figure 3 suggests a method for estimating the effective cathode radius. The procedure consists of employing this analysis together with the experimentally determined voltage and assuming a as an unknown to be determined from the simultaneous solution of the governing equations. Figure 4 shows that the r dependence of V is not as has been assumed in deriving equation (43). It also illustrates the importance of the three-dimensional effects in coaxial devices.

The question arises (also discussed in ref. 8 for the homopolar device) concerning applicability of the theory to light gases where the ion cyclotron radius could be smaller than the electrode gap. For a given mass flow, however, the particle densities will be considerably higher for the lighter gas, a condition which reduces τ_{ia} and somewhat compensates for the effect of increased ω_i on $\omega_i\tau_{ia}$. When ion-neutral collisions are rare, the electrons can still gain energy directly from the electric field over distances smaller than the ion cyclotron radius due to gradients in the potential distribution, whereby the electron conduction may become turbulent. Such a situation exists, for example, for the ionization process in the linear ion Hall accelerator and could also find application for certain range of operations in the present device. Careful distinction must be made between the role of given characteristic parameters for the ionization region and for the region where the acceleration occurs. Thus, especially for the lighter gases, the present ionization mechanism using $T_e > T_i$ may determine the E/B characteristics, and the condition of r_{Li} smaller than the electrode gap may play a role in the acceleration. This problem has to be explored experimentally.

Figure 5 shows a plot of voltage-current characteristics. At the higher currents, both theory and experiment show the existence of a voltage plateau. The theory shows a slightly positive characteristic at the lower currents when the experiment shows a slightly negative characteristic. An explanation for this discrepancy can be attributed to the use of Saha's equation (eq. (13)). Use of Saha's equation with the gas temperature replaced by the electron temperature gives an optimistic estimate of the degree of ionization. Consideration of the various terms in equation (44) shows that, at a given section, it can be approximated by

$$\frac{JV}{\dot{m}} \approx \frac{I}{m}\left(\frac{5}{2}\theta_i + \alpha\right)$$

or

$$V \approx \dot{m}\frac{I}{m}\left(\frac{\frac{5}{2}\theta_i + \alpha}{J}\right) \tag{61}$$

The faster rate of increase of α with J at constant B (see fig. 6) accounts for the slightly positive characteristic predicted by the calculations. It is expected that use of the rate equation, equation (9), in conjunction with the other conservation equations may correct this situation. In this case, the relaxation effects result in a slower increase of α with J at constant B.

This effect may also be attributed to the fact that heat-transfer losses were ignored in the calculations. Such losses would tend to reduce the temperature and, in turn, would reduce α. The voltage-current characteristics must be consistent with those obtained from equation (43) based on the generalized Ohm's law and the momentum equation. The advantage of using the total energy equation is its more general character; however, equation (43) shows dependency on certain parameters which are of great importance in determining the operation of the device.

The experimentally determined Hall current (fig. 7) shows that the Hall current has a maximum. Since $j_\theta = \frac{j_r}{\lambda}$, this behavior is expected because λ consists of two terms, one proportional to B and the other to 1/B; λ is minimum when

$$\frac{1}{\omega_e \tau_{ie}} = 2(1 - \alpha)^2 \omega_i \tau_{ia} \tag{62}$$

The calculations show that the maximum occurs at a higher magnetic field. This condition may be due to the fact that the calculations underestimate the electron temperature (fig. 8). Higher electron temperatures increase $\omega_e \tau_{ie}$ and help bring about the equality in equation (62) at lower magnetic fields.

The possible influence of the measurement technique (see appendix) on the discrepancies between theory and experiment is now discussed. As the magnetic field increases, $\omega_e \tau_{ie}$ becomes larger and the electrons are "tied" more strongly to the magnetic lines. Then the current pattern may bulge further downstream and, as a result, using the same cross-sectional area to calculate j_θ from the total Hall current may introduce some error. Also, if the total current would extend further downstream, the local Hall current probe would only register part of the total current, since the current regions removed from the probe give a smaller signal. Of course, other changes in current patterns also may occur with increasing magnetic field (see also, ref. 4), including the possibility of instabilities that would reduce the Hall current.

Figure 6 shows that the calculations result in a degree of ionization slightly higher than the measured value. As has been explained earlier, use of Saha's equation with the gas temperature replaced by the electron temperature (eq. (13)) leads to optimistic prediction of the degree of ionization.

In spite of the good agreement between theory and experiment one cannot conclude that the use of Saha's equation to calculate the degree of ionization is fully justified. The calculated electron temperature is less than the experimentally measured value. The good agreement between theory and experiment is a result of using this lower temperature in an equation which predicts excessive values for the degree of ionization. The fact that basic trends like the voltage-current characteristics and the voltage-magnetic field characteristics are obtained in spite of these and other approximations suggests that they do not depend on the detailed mechanism of ionization. These results shed some light on the reason for the existence of similar trends of these characteristics for a great variety of operating conditions, as stated in the "Introduction."

In spite of the large scatter of the experimental data (ref. 1), it can still be seen from figure 6 that the rate of increase of α with J is less than that predicted by the theory. This result lends support to the discussion regarding the voltage plateau.

Figure 8 compares the calculated electron temperature with that measured by Langmuir probes for $J = 100$ amperes. The theory underestimates the electron temperature because ionization rates were ignored in the calculations. The interpretation of the measurements of reference 1 showed a discrepancy between probe and spectroscopic measurements. The spectroscopic measurements were made at a point inside the electrode region, whereas probe measurements were made near the tip of the cathode, outside the electrode region. Because of this, some discrepancy is expected. However, a recent reevaluation of the spectroscopic data of reference 1 at the Langley Research Center brought the spectroscopic measurements in line with the probe measurements. When operating at 200 amperes in the presence of argon lines AI and AII, the AII lines being more intense, an electron temperature in the range of 14 000° K to 20 000° K has been

estimated. This value is in good agreement with the probe measurements at 200 amperes, which ranged from 14 000° K to 18 000° K. Further discussion of the spectroscopic measurements is given in the appendix.

CONCLUDING REMARKS

The theory presented here is based on the conservation equations of the plasma constituents and does not assume that the ions are orbiting with E/B drift velocity where E is the electric field strength and B is the magnetic field strength. It predicts the linear voltage-magnetic field strength characteristics at constant current observed by the various investigators and indicates the existence of a voltage plateau for a constant magnetic field at the higher currents.

It is shown that an ionization mechanism based on electron temperatures in excess of ion temperatures is responsible for the observed characteristics. This result is in contrast to the mechanisms proposed by Alfvén and used by Lin, Patrick, and Schneiderman.

The model employed here predicts fairly well the gross characteristics of the coaxial Hall current accelerator.

It is evident from the discussion, however, that relaxation effects play an important role in crossed field discharges. This conclusion is reached in spite of the fact that various effects seem to counteract each other with the result that reasonable agreement is obtained by using Saha's equation. It is concluded that, for a better understanding of the ionization and acceleration processes, a more elaborate analysis, which takes into consideration relaxation and three-dimensional effects is required. The fact that for the approximations made, the basic trends, like the voltage-current characteristics and the voltage-magnetic field strength characteristics, were obtained in spite of these and other approximations is, however, in itself a significant result. The result suggests that these basic trends do not depend on the detailed mechanism of ionization and distribution of power in the plasma. This behavior helps to explain the existence of similar trends of these characteristics for a great variety of operating conditions.

North Carolina State University, Raleigh, N. C.
and Langley Research Center,
National Aeronautics and Space Administration,
Langley Station, Hampton, Va., July 8, 1966.
129-01-05-04-23

APPENDIX

DISCUSSION OF SPECTROSCOPIC AND HALL CURRENT MEASUREMENTS

Spectroscopic Measurements

Electron temperature determinations in the coaxial accelerator were made from identification of the emitted spectra lines rather than from relative line intensities. Since spatial nonuniformities exist in the plasma, and spatial resolution could not yet be achieved, complete knowledge of where the emitted spectral lines originate is not possible. Thus the relative line intensity method may give an incorrect temperature based on lines from different regions. The line identification method, however, yields correct information of the range of temperatures over the entire radial region. For a spatially uniform plasma, both methods should produce the same results.

Both methods of electron temperature measurement are valid only in a steady state. Calculations indicate that the residence time of a particle in the accelerator is shorter than the time required to reach steady-state ionization. Thus, if the equilibrium state can be expected to occur at higher T_e, the electron temperature measurements are a lower limit, since the temperature is still increasing as a typical plasma volume element leaves the region under observation.

Three radial positions of the electrode region were observed in the measurements. Access to the electrode region was achieved by drilling three parallel holes through the anode body and anode ring and inserting three stainless-steel tubes through the body up to the anode ring. With the line of sight through the tubes and the holes in the anode ring, the three radial positions between the anode and cathode could be observed. These radial positions were (1) a position just off the cathode surface, (2) one just off the anode wall surface, and (3) one which is half the distance between the cathode and anode walls.

Spectrograms were obtained from each of the three regions at various magnetic fields and arc currents, and the films were scanned with a microdensitometer. The traces showed that the most intense lines were emitted from the center tube and the weakest lines from the region nearest the anode wall. The lines were identified and the electron temperature was determined from the presence of the lines by two methods. In one method the Saha equation, corrected for low density conditions, was used to find the variation of the relative population of the argon ground states with electron temperature. In the other method, the intensities of several observed excited AI and AII lines compared with electron temperature tabulated by Oertel and Raiford were used. Although the method using the excited lines is more accurate, reasonable agreement was found with the ground

state method, and the range of electron temperatures was found to be from 14 000° K to 20 000° K, when operating at 200 amperes. As mentioned previously, this limit is the lower limit of temperature. The upper end of the temperature range appears to be in the center position with the temperature decreasing toward the anode wall and the cathode. Determination of the true radial temperature distribution would require use of an Abel inversion.

For the electron density measurements, Stark broadening of the H_β line was used. This measurement yielded only an order of magnitude estimate of the density. This method is suited to electron densities of 10^{16} to 10^{18} electrons per cubic centimeter, whereas at low densities, around 10^{14} electrons per cubic centimeter, the plasma line profile is of the order of the instrument profile, and thus interferes with accurate measurements. It is estimated that the accuracy of the electron density measurements used in this method are not much better than ±50 percent.

Hall Current Measurements

The Hall current was measured by placing a search coil around the plasma stream, the coil being embedded in a boron nitride nozzle immediately adjacent to the copper anode ring. The Hall current signal is obtained by "crowbarring" the arc current into a resistor load, and thereby obtaining a clean arc shutoff. The collapsing Hall magnetic field then induces an electromotive force and current in the coil; the charge obtained by integration of this current in a ballistic galvanometer is proportional to the Hall current in the plasma. The calibration of the Hall current was performed by placing a small many-turn coil in the approximate position where the Hall current was thought to be largest.

The Hall current measurements were obtained in amperes, and the Hall current is assumed to be distributed in a single-turn loop. To permit comparison with the theoretical values of Hall current density j_θ the Hall currents were divided by a constant cross-sectional area with the height of the 0.76-cm electrode gap and with an assumed discharge length of 1 cm.

REFERENCES

1. Grossmann, William, Jr.: Theory and Experiment of a Co-Axial Plasma Accelerator. Ph.D. Thesis, Virginia Polytech. Inst., May 1964.

2. Grossmann, William, Jr.; Hess, Robert V.; and Hassan, H. A.: Experiments With a Coaxial Hall Current Plasma Accelerator. AIAA J., vol. 3, no. 6, June 1965, pp. 1034-1039.

3. Cann, G. L.; and Harder, R. L.: Follow-on Investigation of a Steady State Hall Current Accelerator. NASA CR-54062, 1964.

4. Patrick, R. M.; and Schneiderman, A. M.: Performance Characteristics of a Magnetic Annular Arc. Sixth Symposium on Engineering Aspects of Magnetohydrodynamics, Univ. of Pittsburgh, Apr. 1965, pp. 70-82.

5. Alfvén, H.: Collision Between a Nonionized Gas and a Magnetized Plasma. Rev. Mod. Phys., vol. 32, no. 4, Oct. 1960, pp. 710-713.

6. Hess, Robert V.: Fundamentals of Plasma Interaction With Electric and Magnetic Fields. Proceedings of the NASA-University Conference on the Science and Technology of Space Exploration, vol. 2, NASA SP-11, 1962, pp. 313-336.

7. Lin, Shao-Chi: Limiting Velocity of a Rotating Plasma. The Physics of Fluids, vol. 4, no. 10, Oct. 1961, pp. 1277-1288.

8. Dobryshevskii, É. M.: The Volt-Ampere Characteristics of a Homopolar Cell. Soviet Phys.-Tech. Phys., vol. 8, no. 10, Apr. 1964, pp. 903-905.

9. Hassan, H. A.: Nonequilibrium Ionization in the Presence of Electric and Magnetic Fields. Fourth NASA Intercenter Conference on Plasma Physics. NASA, Dec. 1963, pp. 69-73.

10. Hassan, H. A.; Hess, R. V.; Grossmann, W.; Brockman, P.; and Oertel, G.: Experiments and Analysis for Coaxial Hall Current Accelerators and the Role of Ionization Effects. Sixth Symposium on Engineering Aspects of Magnetohydrodynamics, Univ. of Pittsburgh, Apr. 1965, pp. 83-84.

11. Burgers, Johannes M.: Statistical Plasma Mechanics. Ch. 5 of Plasma Dynamics, Francis H. Clauser, ed., Addison-Wesley Publ. Co., Inc., c.1960, pp. 119-186.

12. Kerrebrock, Jack L.: Conduction in Gases With Elevated Temperature. Engineering Aspects of Magnetohydrodynamics, Clifford Mannal and Norman W. Mather, eds., Columbia Univ. Press, c.1962, pp. 327-346.

13. Chapman, Sydney; and Cowling, T. G.: The Mathematical Theory of Non-Uniform Gases. Cambridge Univ. Press, 1960.

14. Cowling, T. G.: Magnetohydrodynamics. Interscience Publ. Inc., 1957.

15. Spitzer, Lyman, Jr.: Physics of Fully Ionized Gases. Second rev. ed., Interscience Publ., Inc. (New York), 1962.

16. Massey, H. S. W.; and Burhop, E. H. S.: Electronic and Ionic Impact Phenomena. The Clarendon Press (Oxford), 1952. (Reprinted 1956.)

17. Barbiere, Domenick: Energy Distribution, Drift Velocity, and Temperature of Slow Electrons in Helium and Argon. Phys. Rev., Second ser., vol. 84, no. 4, Nov. 15, 1951, pp. 653-658.

18. Frost, L. S.; and Phelps, A. V.: Momentum Transfer Cross Sections for Electrons in Argon. Bull. American Phys. Soc., ser. II, vol. 6, no. 1, Feb. 1, 1961, p. 371.

19. Fay, James A.: Hypersonic Heat Transfer in the Air Laminar Boundary Layer. Ch. 30 of The High Temperature Aspects of Hypersonic Flow, Wilbur C. Nelson, ed., Pergamon Press, 1964, pp. 583-604.

20. Hirschfelder, Joseph O.; Curtiss, Charles F.; and Bird, R. Byron: Molecular Theory of Gases and Liquids. John Wiley & Sons, Inc., c.1954.

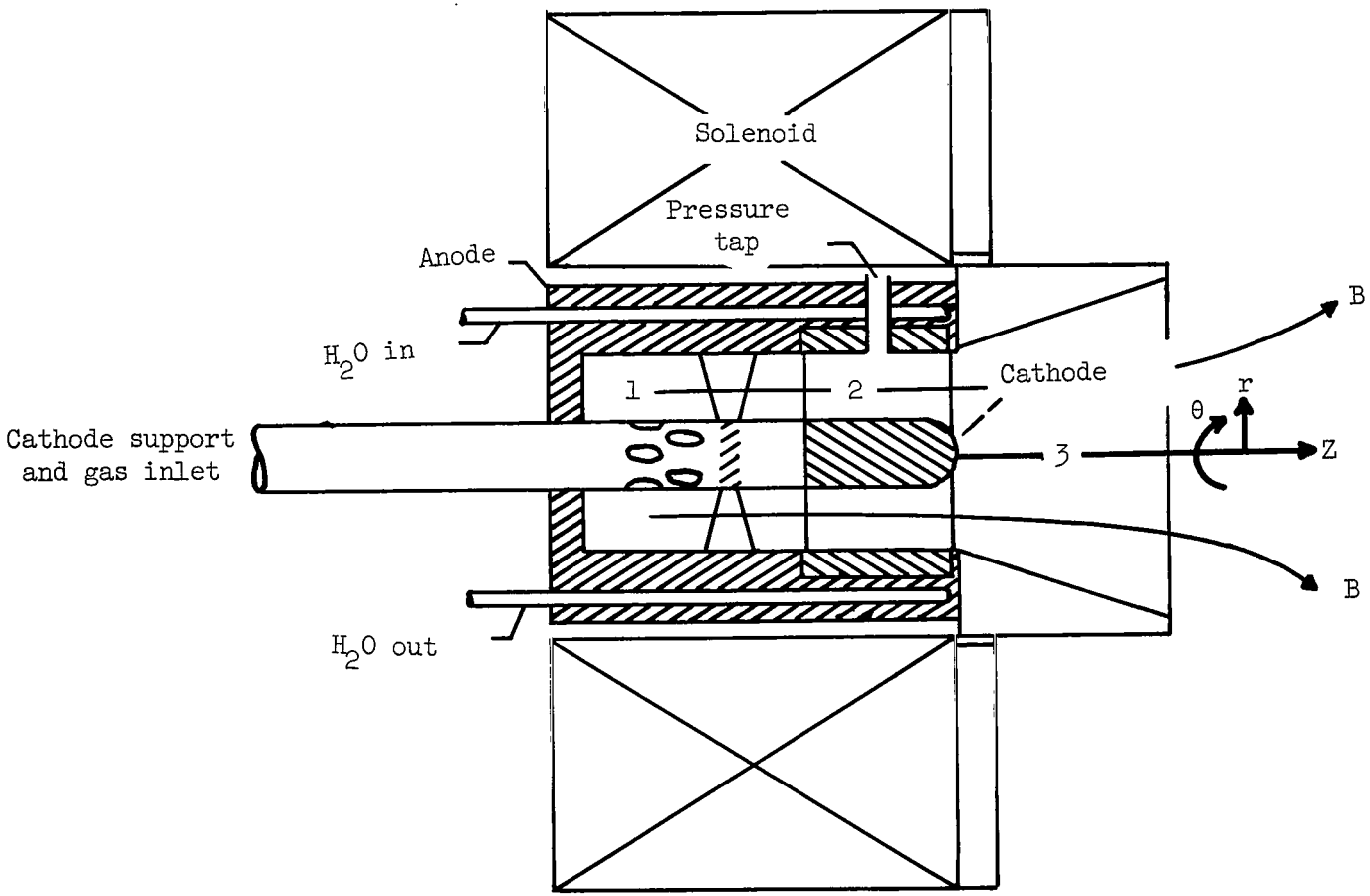

Figure 1.- Schematic diagram of accelerator.

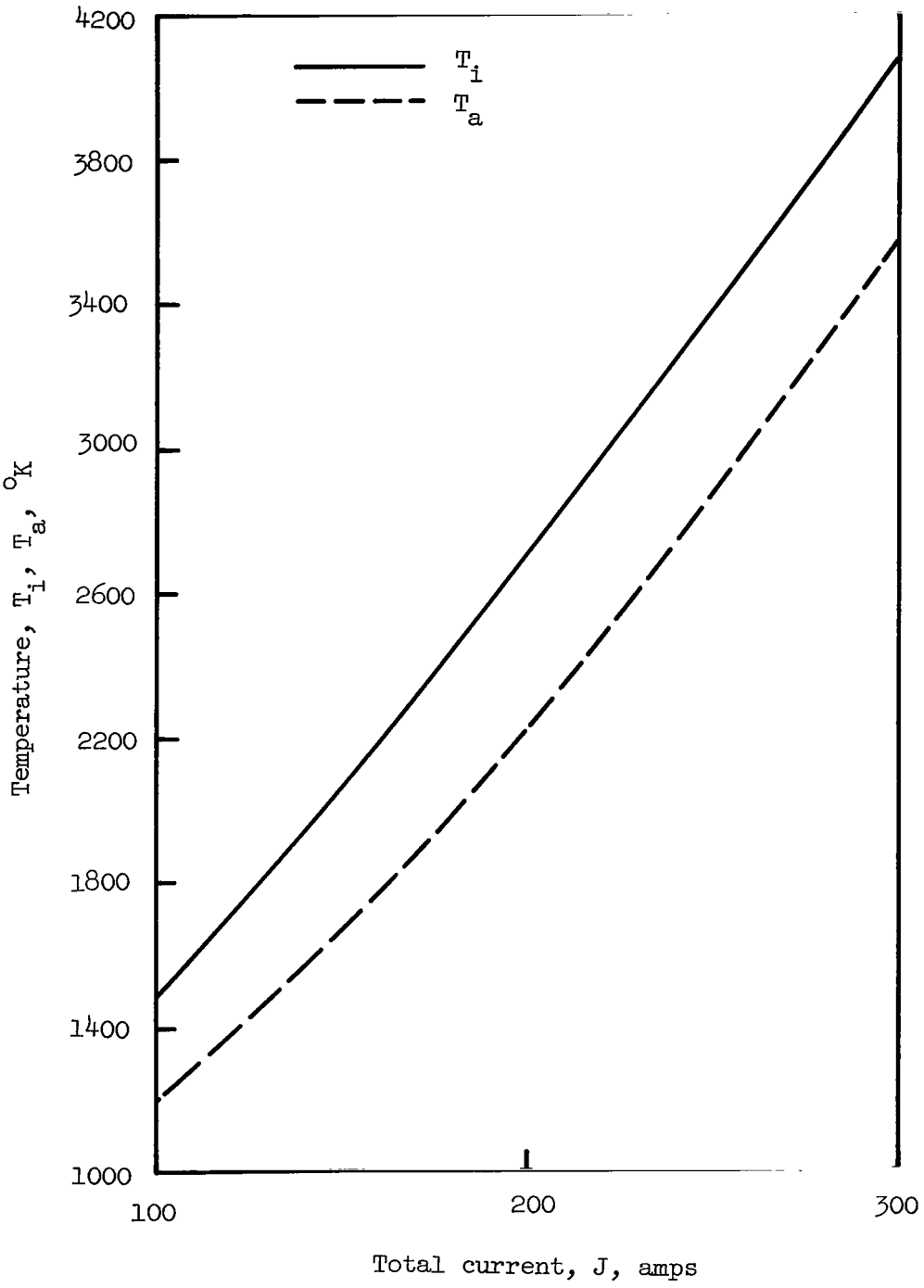

Figure 2.- Variation of theoretical prediction of ion and neutral temperatures with total current. B = 3000 gauss.

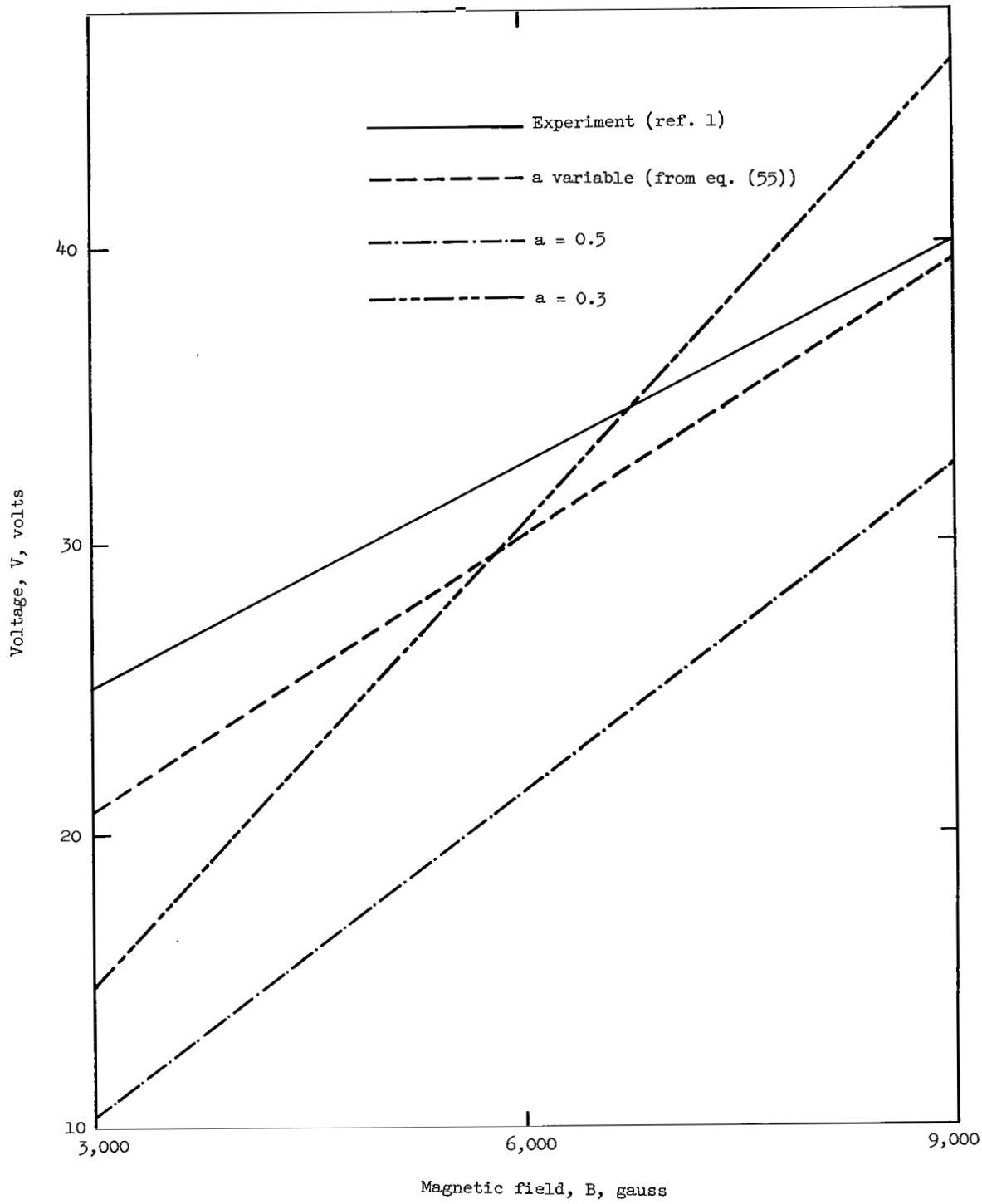

Figure 3.- Variation of voltage with magnetic field for given r. J = 100 amperes; r = 1.2.

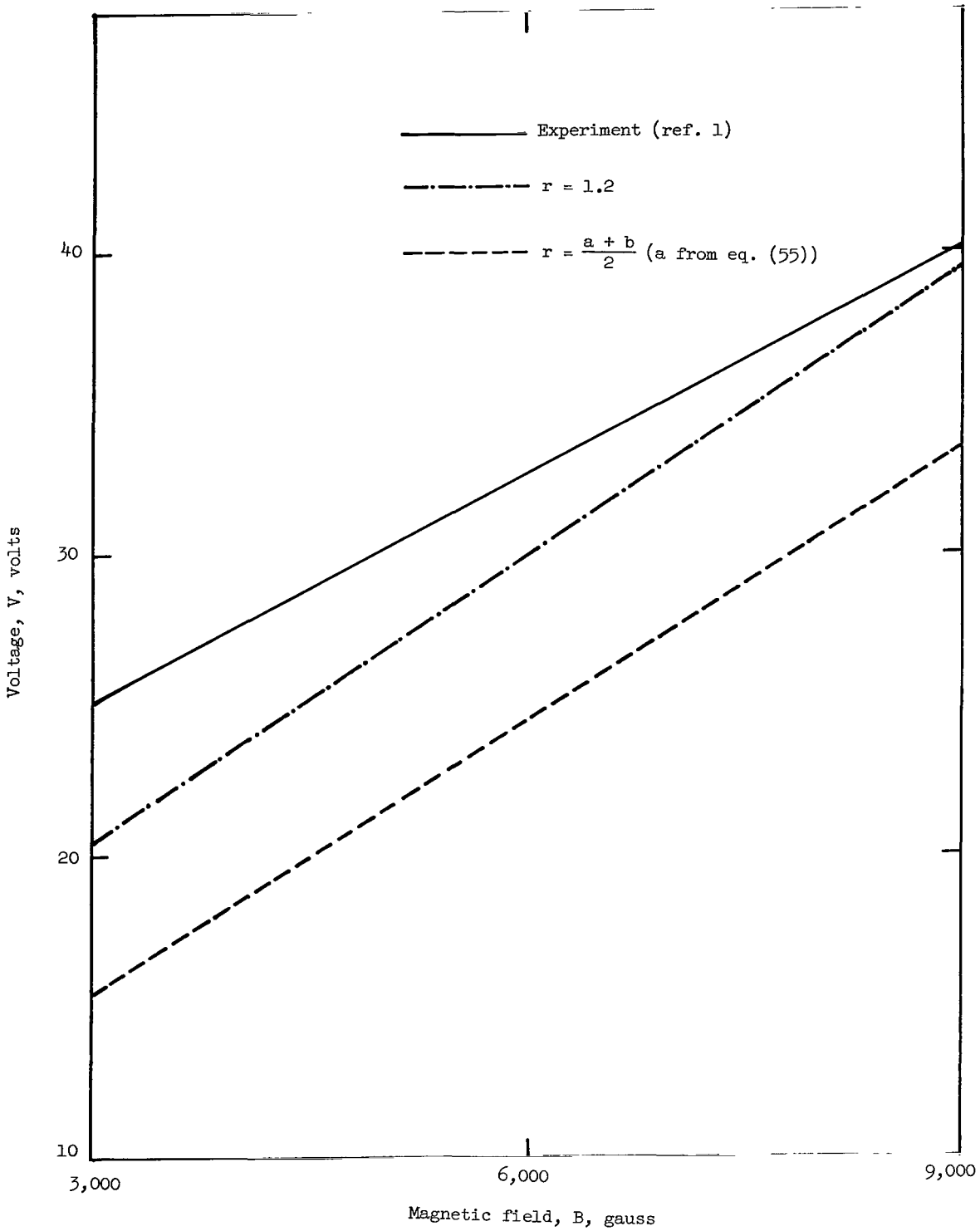

Figure 4.- Comparison of theory and experiment. Variation of voltage with magnetic field for varying r. J = 100 amperes.

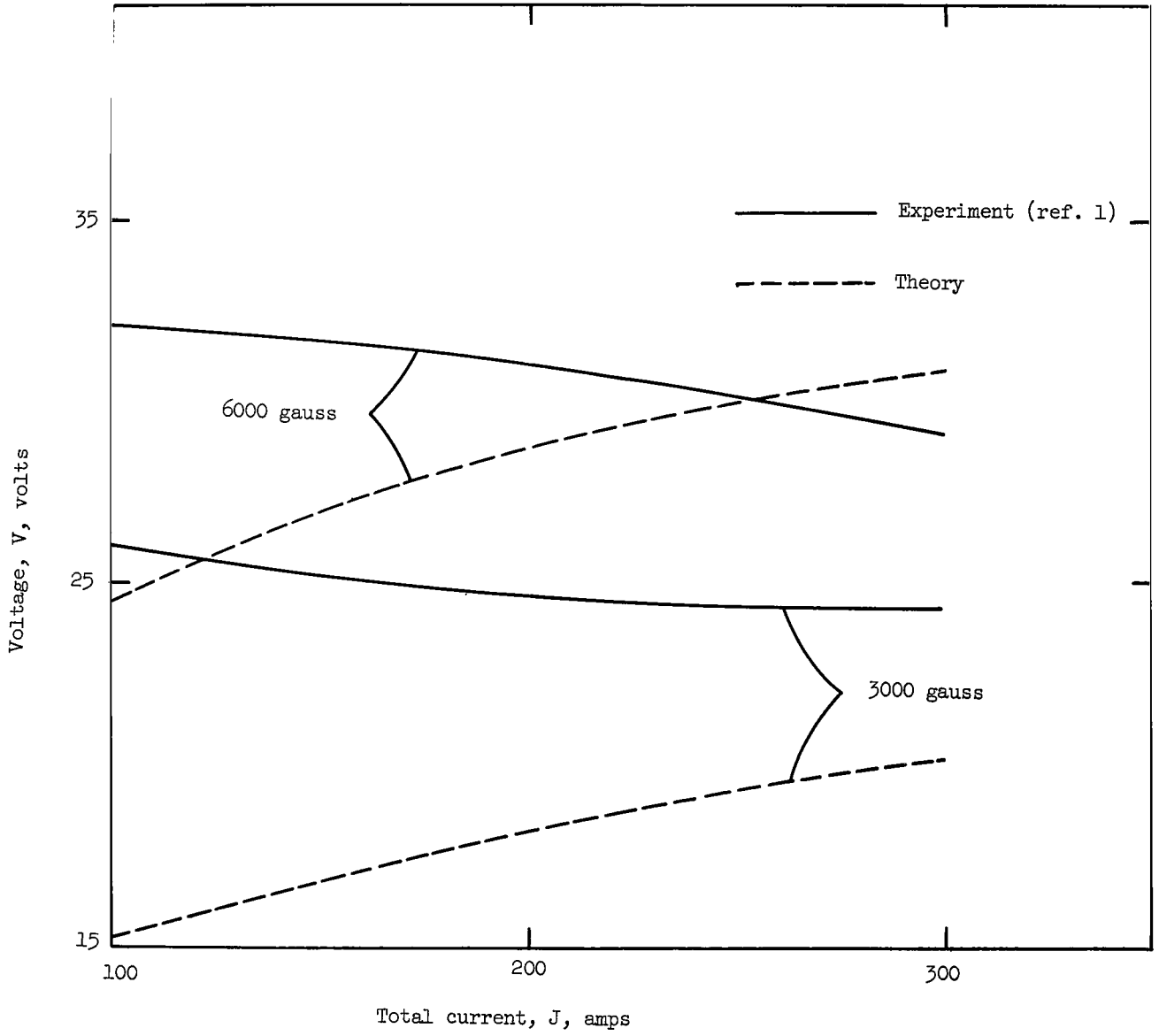

Figure 5.- Comparison of theory and experiment. Variation of voltage with total current.

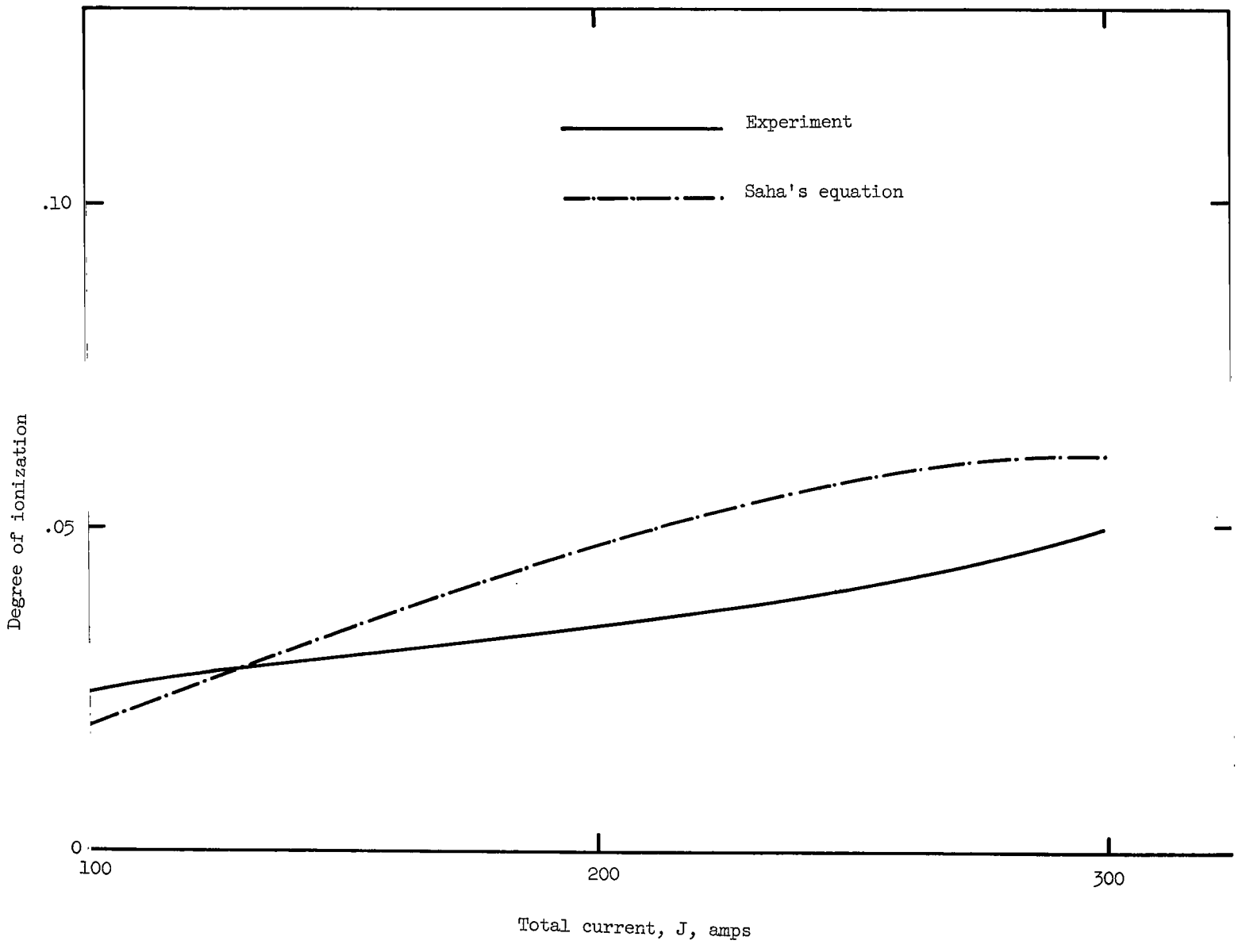

Figure 6.- Comparison of theory and experiment. Variation of degree of ionization with total current. B = 6000 gauss.

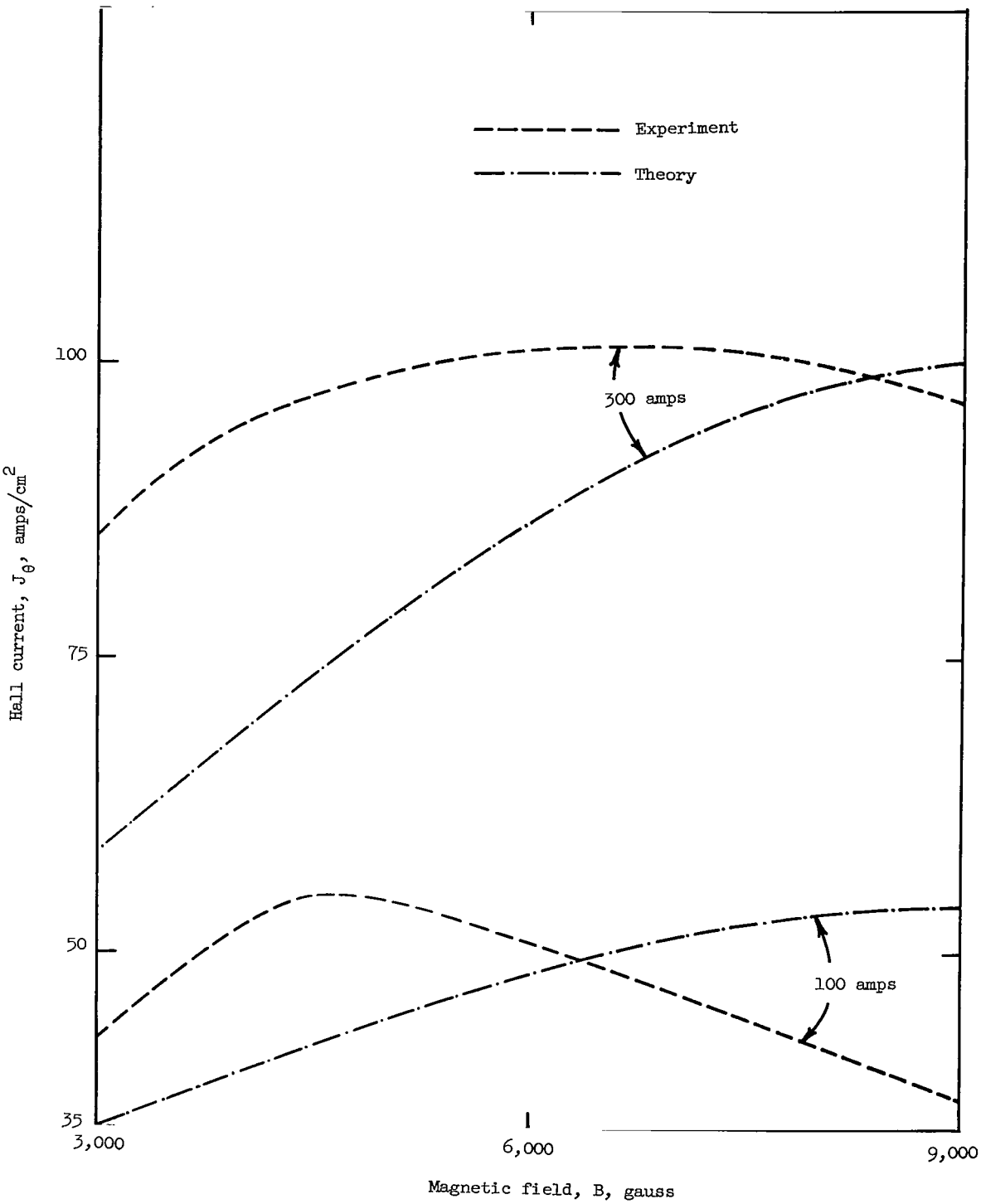

Figure 7.- Comparison of theory and experiment. Variation of Hall current with magnetic field.

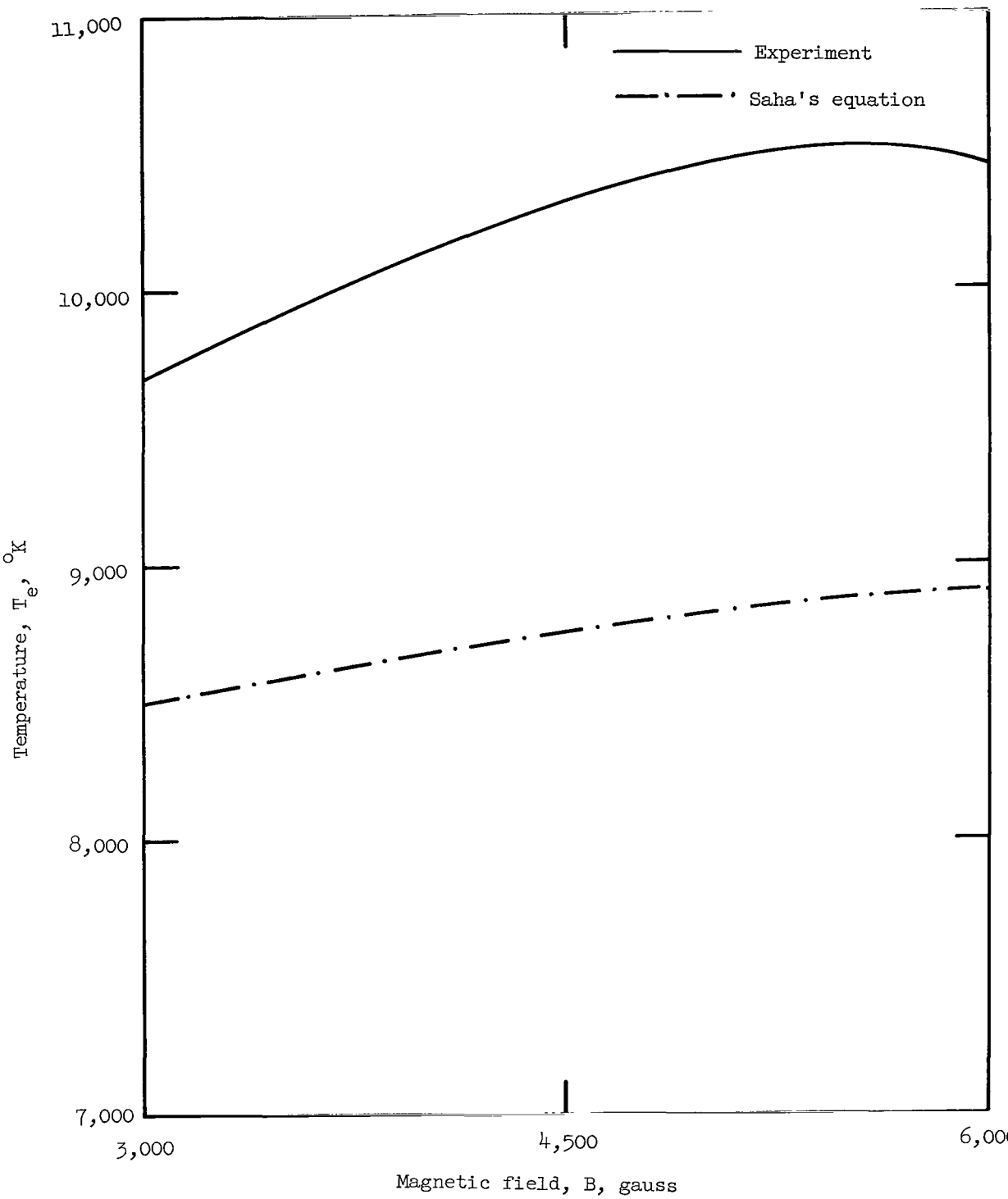

Figure 8.- Comparison of theory and experiment. Variation of electron temperature with magnetic field. J = 100 amperes.

NASA-Langley, 1966 L-3713

"The aeronautical and space activities of the United States shall be conducted so as to contribute . . . to the expansion of human knowledge of phenomena in the atmosphere and space. The Administration shall provide for the widest practicable and appropriate dissemination of information concerning its activities and the results thereof."

—NATIONAL AERONAUTICS AND SPACE ACT OF 1958

NASA SCIENTIFIC AND TECHNICAL PUBLICATIONS

TECHNICAL REPORTS: Scientific and technical information considered important, complete, and a lasting contribution to existing knowledge.

TECHNICAL NOTES: Information less broad in scope but nevertheless of importance as a contribution to existing knowledge.

TECHNICAL MEMORANDUMS: Information receiving limited distribution because of preliminary data, security classification, or other reasons.

CONTRACTOR REPORTS: Technical information generated in connection with a NASA contract or grant and released under NASA auspices.

TECHNICAL TRANSLATIONS: Information published in a foreign language considered to merit NASA distribution in English.

TECHNICAL REPRINTS: Information derived from NASA activities and initially published in the form of journal articles.

SPECIAL PUBLICATIONS: Information derived from or of value to NASA activities but not necessarily reporting the results of individual NASA-programmed scientific efforts. Publications include conference proceedings, monographs, data compilations, handbooks, sourcebooks, and special bibliographies.

Details on the availability of these publications may be obtained from:

SCIENTIFIC AND TECHNICAL INFORMATION DIVISION

NATIONAL AERONAUTICS AND SPACE ADMINISTRATION

Washington, D.C. 20546